INFORMATION FROM DEEP-SPACE TRACKING

Close inspection of spacecraft orbits has yielded a surprising amount of data on masses, radii, atmosphere and gravity of the moon and some planets and most recently lunar mascons.

PAUL M. MULLER and WILLIAM L. SJOGREN

THE REMARKABLE NAVIGATION feats of the US deep-space probes were accomplished because of the farsighted attitude assumed in the development of a radio tracking system at the Jet Propulsion Laboratory. It was probably not fully realized at the outset what an enormous amount of scientific information would eventually be extracted from the data.

The best estimates today on the masses of Mars, Venus, earth and the moon, the radius of Mars and the moon, the relative locations of our continents, some atmospheric properties of Mars and Venus and the position and gravity field of the moon have all been determined fundamentally from direct processing of data produced by the Doppler and ranging system during Ranger, Surveyor, Lunar Orbiter, Pioneer and Mariner spacecraft flights. The accuracy of the data can be judged from the unexpected detection of "mascons," or local mass concentrations, on the moon (figure 1), for which small variations in spacecraft speed of about 50 mm/sec were separated from the average orbital speed of 2×10^6 mm/sec. Even those of us who use and process these data are continually amazed at their accuracy and are only now at the point where we can evaluate some of the more subtle system-error characteristics.

Doppler tracking

The radio tracking system in a simplified form is a phase-coherent loop. Coherent detection involves establishing local signal timing in step with a multiple or submultiple of the transmitted carrier frequency; hence, it establishes a local phase identity with the transmitted signal. The phase-coherent loop includes earth-based transmitting and receiving radio antennas with their many assorted diplexers, phase detectors, synthesizers and oscillators, plus the spacecraft's transponder that coherently retransmits the signal received from earth. The tracking system, however, is encompassed by the Deep Space Network, which consists of an operations facility at JPL, a ground communications network and five primary tracking sites.[1] There are three 25-meter antennas and a 63-meter antenna at Goldstone, California, two of 25 meters at Madrid, Spain and single 25-meter antennas at Johannesburg, South Africa, and at Woomera and Canberra, Australia. With these fully steerable parabolic dishes, continuous coverage can be maintained with spacecraft that have traveled more than about 15 000 km from the earth.

Figure 2 is a schematic representation of the Doppler tracking system, showing how a signal is transmitted to the spacecraft (nominally on the S band). This signal is retransmitted by the spacecraft on an altered but coherent frequency. It is then received at the ground station and compared with the atomic-oscillator signal from which the transmission frequency was derived. Simple comparison of the transmitted and received signals yields the Doppler shift imposed upon the signal during the round-trip path between station and spacecraft. Addition of a 1-MHz bias results in positive numbers for the Doppler shift. The cumulative count of Doppler cycles is stored on paper and magnetic tape for later processing. These raw data contain the line-of-sight range-change information over the selected time interval. By averaging over the desired sample time, a mean range rate V_r can be cal-

Paul M. Muller is a senior research engineer in the systems analysis research section at Jet Propulsion Laboratory. After receiving his BA from San Fernando State College in 1960 and teaching for three years, he joined JPL in 1964. Recently he has become interested in lunar-data analysis and was codiscoverer with Sjogren of lunar mascons. He is now doing further investigations of lunar history.

William L. Sjogren joined the Jet Propulsion Laboratory in 1962 after receiving his MS from Northwestern University. He is now a member of the technical staff in the systems analysis research section. Sjogren has worked on the navigational aspects of all the lunar projects and has done postflight analysis of their data, providing determination on physical constants, the latest being the lunar gravity field.

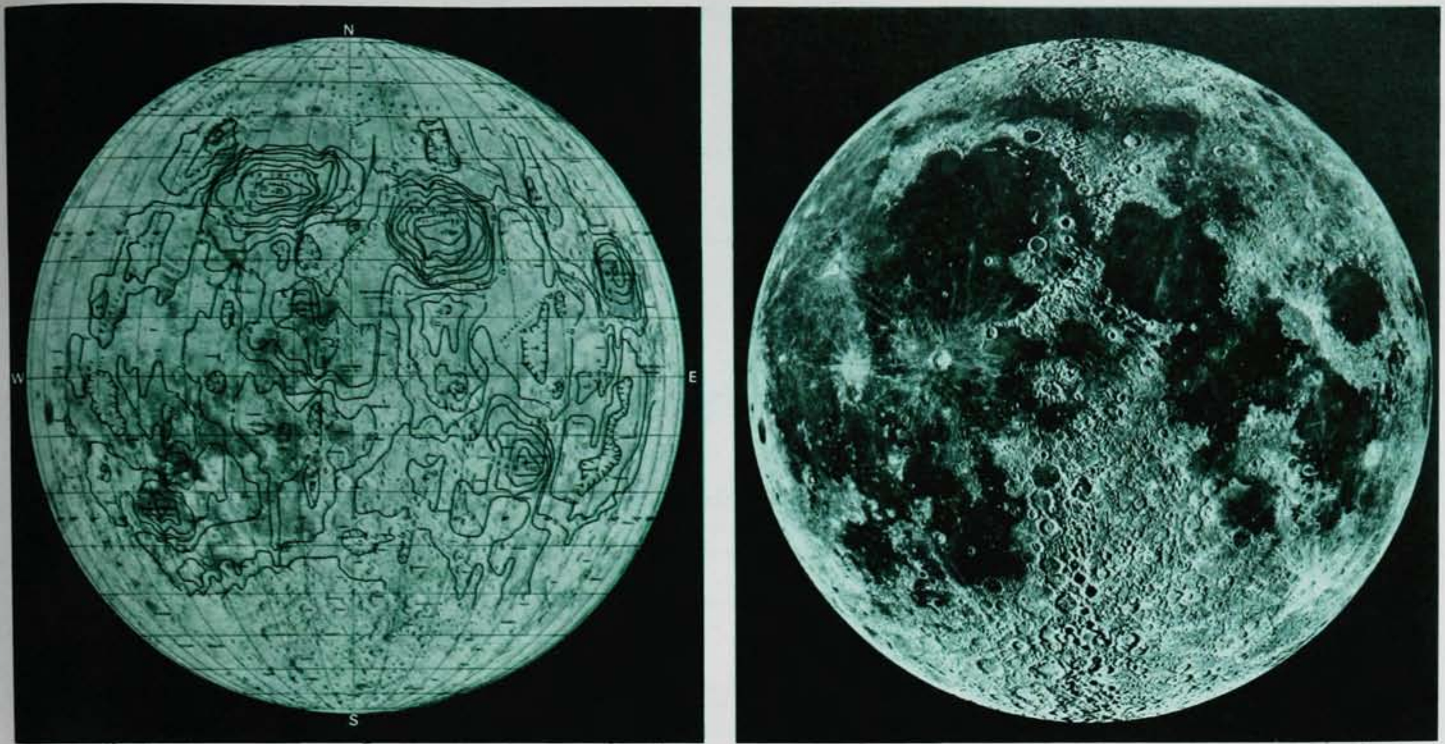

MASS CONCENTRATIONS (mascons) on the moon. This gravimetric map (left) was made from 74 consecutive orbits of Lunar Orbiter. Note the correlation between the mascons, 10 of which are now verified, and the ringed seas. Unretouched composite photo on right is for comparison. —FIG. 1

culated to first-order accuracy by the expression shown in figure 2. V_r is only a concept, for $\int_0^T V_r\, dt$ is the Doppler observable, and it is the quantity theoretically calculated by the computer program. The Doppler-observable calculation can also be performed by a simple difference calculation.

Three very significant features of the system should be mentioned. First the rubidium frequency standard generates the transmitted frequency as well as the reference standard with which the received signal is compared to produce Doppler data. They are stable to about 2.5 parts in 10^{12} and this stability is one of the prime factors in reducing the data noise. Second, continuously accumulating the cycle count permits greater flexibility and economy in data processing, such as data compression or the detection of long-period secular effects. The consequent saving in computation time is desirable, and the high-frequency noise effect is reduced as well. The third feature is the resolver used in the output-sampling circuits. This device detects the fractional part of a cycle count to approximately 0.01 cycles (where 1 cycle = 65 mm) and has considerably improved the accuracy of high sample-rate data. Previously many small short-period systematic errors had been masked in the noise. For example the Pioneer spin rate was extracted with a power-spectra analysis, and Mariner 4 occultation data were enhanced.

Limiting errors

Within the last two years the limiting error sources of this system have been thoroughly analyzed. Before this time the limitations of the computer programs and our understanding of the basic relevant physical parameters had kept the hardware accuracy well ahead of the modeling and computation accuracy. As we close the gap, the hardware-system engineers are putting in

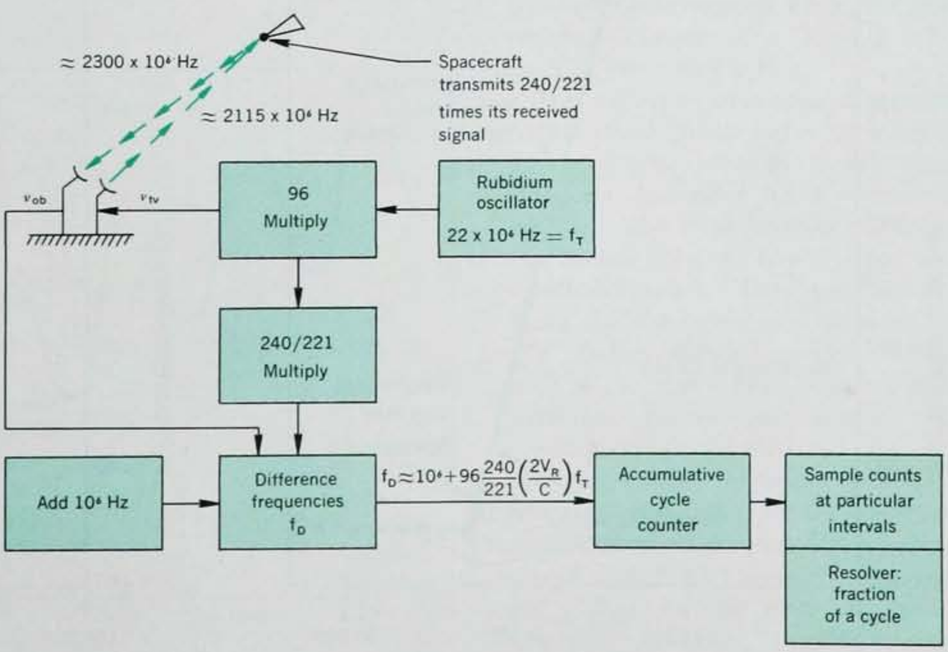

DOPPLER TRACKING SYSTEM, showing schematically how the spacecraft retransmits the received signal on an altered but coherent frequency. Comparison with the rubidium oscillator frequency reveals the Doppler shift, from which line-of-sight range change can be derived. Oscillator is stable to 2.5 parts in 10^{12}. —FIG. 2

cesium and hydrogen masers for improved oscillator stability and improved counters for reliability. Donald W. Trask at JPL has suggested an approximate empirical formula to describe the high-frequency noise on a data sample

$$\sigma_{\Delta r}^2 = (3.0)^2 + (3.5\sqrt{T_{min}})^2$$

where $\sigma_{\Delta r}^2$ is the variance on a range change over the count time in mm^2 and T_{min} is the minimum of the round-trip signal time or the count interval time in seconds. The first term in the expression represents the contribution by all known and unknown physical parameters outside the transponder equipment. This contribution includes such things as short-term noise introduced by the atmosphere, ionosphere, space-plasma and other unknown effects not covered elsewhere. The second term covers the rubidium-oscillator stability factor previously mentioned. When the sample rate is high (1 per second) the oscillator stability is comparable to the other error sources and could conceal their presence.

For absolute range measurements rather than range differences the Lunar Orbiter and Mariner 1967 spacecraft provided data with 1-meter and 8-meter high-frequency noise and 15-meter and 50-meter biases respectively.

With the installation of hydrogen masers, the stability could reach 1 part in 10^{13}, and further characteristics of existing errors could be effectively analyzed and included in the theoretical model, which has already grown to enormous proportions. It now includes, for example, such things as wandering of the earth's pole, charged particles, troposphere, oblateness of Mars and Venus, variations in Universal Time, plus the effects of general relativity, all because the tracking

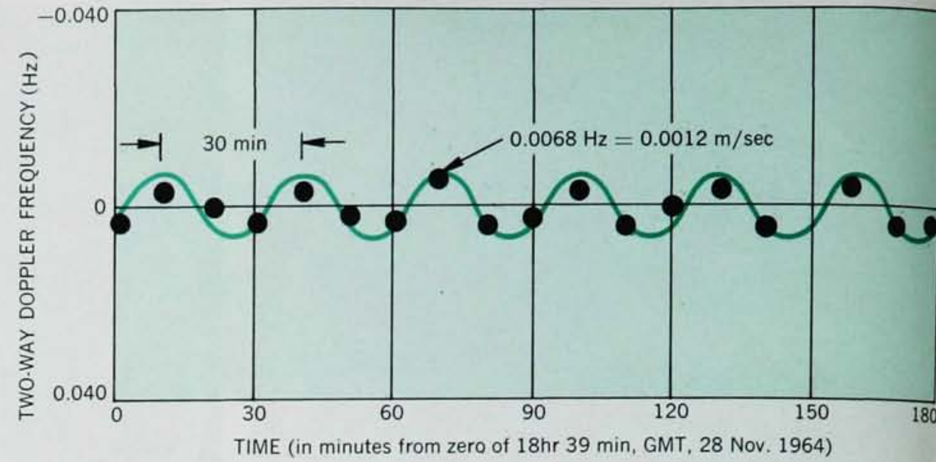

TUMBLING of Mariner 4 shown by the Doppler residuals. Actual data taken on 28 Nov. 1964, with the spacecraft at a range of about 61 000 km, are shown by black dots. Colored line is a result of the theoretical calculation. —FIG. 3

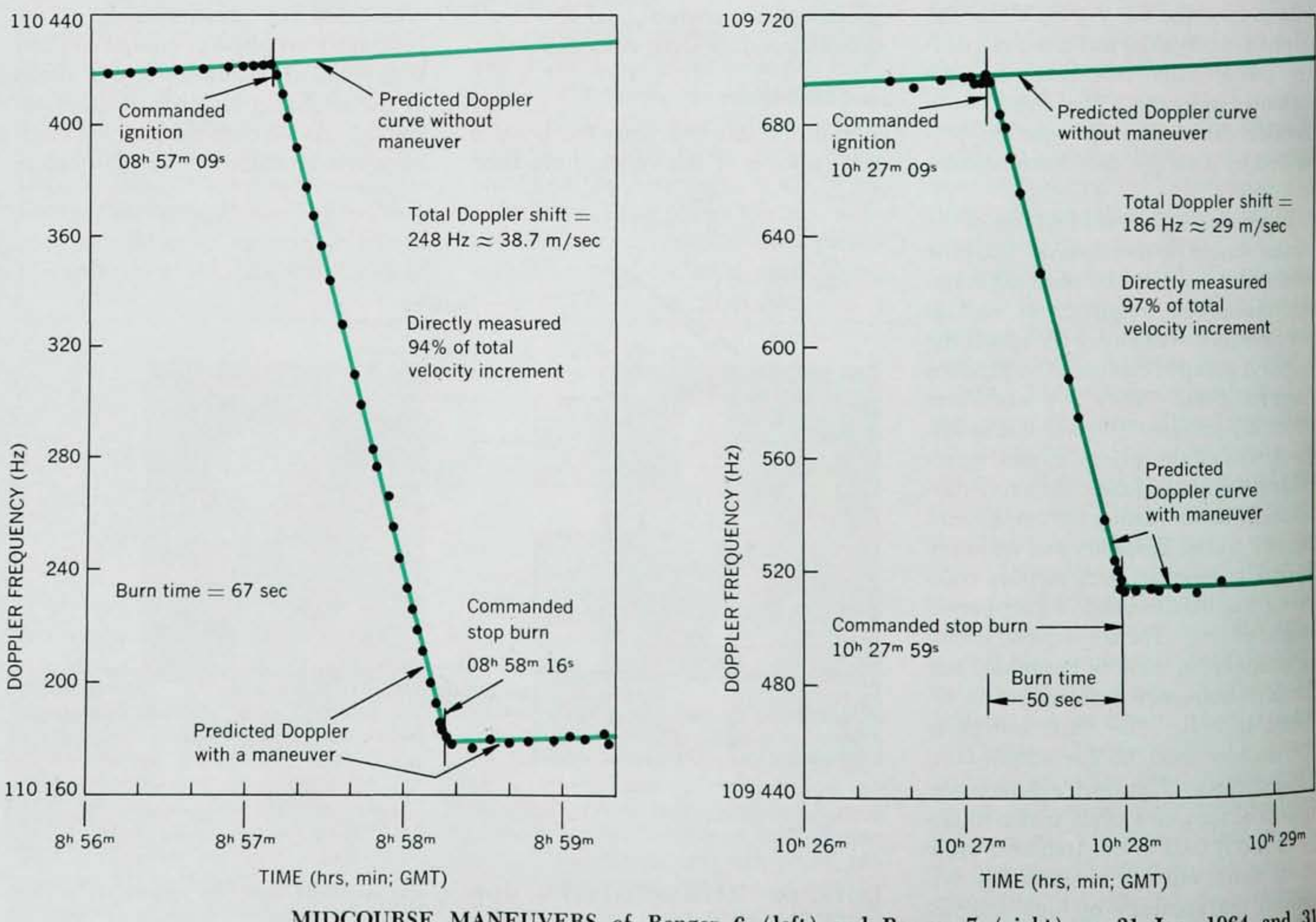

MIDCOURSE MANEUVERS of Ranger 6 (left) and Ranger 7 (right) on 31 Jan. 1964 and 31 July 1964, respectively. Comparison of real data (black dots) with prediction (colored lines) reveals that the maneuvers were properly performed. —FIG. 4

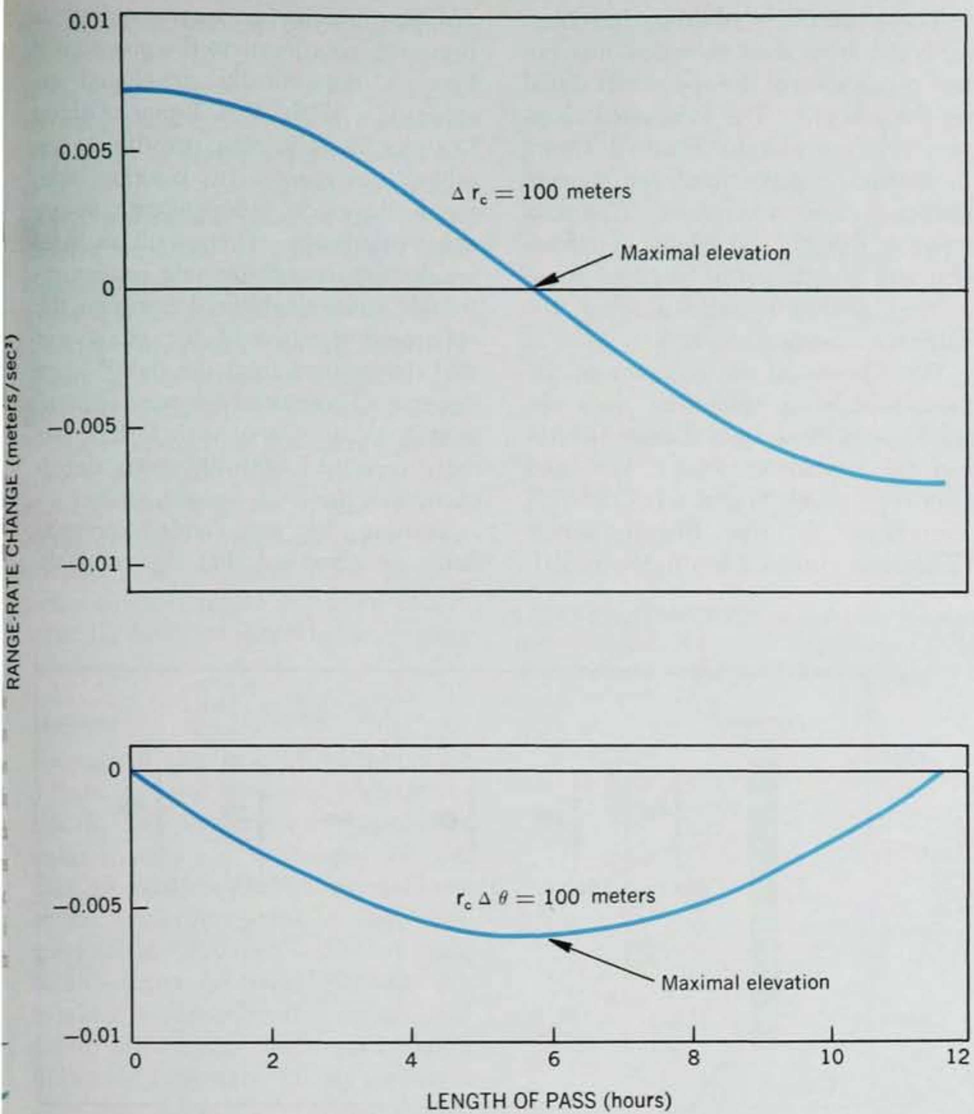

STATION LOCATION ERROR. Upper graph shows result of an error in that component of station location that is the distance from the earth spin axis. Lower graph is the error in range rate caused by an error in longitude. —FIG. 5

PERIODIC MOTION of the earth around the earth–moon center of gravity causes this periodic variation in Mariner 4 data. This variation determines *GM*, the product of gravitational constant and mass, for the moon. —FIG. 6

data are sensitive to these variations at the level of accuracy achievable.

The navigational capability of the theoretical model with the present Doppler data is 250-km 3-σ position uncertainty at a Mars encounter. However, in the 1970's, with new cesium or hydrogen masers as oscillator standards and improved theoretical models (primarily the ephemerides), it is anticipated that position accuracies of 50–100 km will be achieved at Mars, 200–300 km at Jupiter, and approximately 1000 km at Uranus. These accuracies are within the fuel requirements for the grand-tour mission to the outer planets.

Information extraction

A host of parameters has been determined from analysis of the radio-tracking data. We shall now discuss some of the more dramatic ones, indicating how they became evident.

During the real-time navigation of any deep-space mission many spacecraft events can be directly verified by observing the Doppler residuals. The residuals are defined to be the difference between what is actually observed and what is theoretically calculated for the spacecraft motion by the model. For example, figure 3 shows the tumbling of Mariner 4 before its onboard sensor acquired the star Canopus and achieved inertial stability. The period of rotation is easily computed, as is the actual distance of the spacecraft antenna with respect to the center of gravity. The time of acquisition is determined when the systematic signature stops, leaving only the high-frequency noise.

The midcourse maneuver is a very critical event, for its motor burn trims the spacecraft orbit to the precise aiming point demanded for a successful mission. The Doppler residuals from two Ranger missions to the moon are shown in figure 4. There can be little doubt that the motor performed properly. In fact, detailed postflight analysis[2,3] of the motor burn revealed and permitted precise measurement of pointing errors and detected a slight overburn. Many anomalies in a mission are first detected by the tracking-data residuals and result in investigation of a particular system or maneuver. They include such effects as spacecraft gas leaks, tracking-station malfunction, input errors to the computer and timing errors.

In the postflight analysis of the data more subtle, yet quite conspicuous, effects can be seen. As a result, the JPL tracking system has produced the best determined values for many physical parameters.[4] We now have locations of tracking stations to an accuracy of 5 meters and better. Previous determinations were in error in some cases by as much as 150 meters, as has been verified by earth-satellite data of an intermediate precision.[5] Independent solutions for the relative locations of the Goldstone stations from geodetic survey and spacecraft missions agree to within 2 meters in the worst case. With independent checks of this kind, we build considerable confidence in the results. We should note that only two components of position in these location determinations can be found from deep-space probe data. They are longitude and distance from the earth's spin axis. The direction parallel to the earth's spin axis is obtained from the complementary earth-satellite data, completing the solutions. This coördinate is important only for situations relatively near the earth—say to lunar distance.

The characteristic signature of a station-location error in the residuals is shown in figure 5. Station-location information is of primary concern in earth-based space navigation, for errors of 5 meters translate into miss distances of a hundred km at Mars and a thousand km at Jupiter.

Mass of the moon

The gravitational attraction of the moon is another parameter that has been uniquely and independently determined from different tracking-data reduction techniques. We measure it in terms of *GM*, the product of the universal gravitational constant and mass. These new estimates of *GM* are two orders of magnitude better than the previously determined values[6] (that is, past 4900.0 ± 5.0 km^3/sec^2, present 4902.78 ± 0.05 km^3/sec^2). The Mariner-2 and 4[7,8] data determined this parameter from the 28-day periodic motion of the earth about the barycenter of the earth–moon system (figure 6). As we already knew the earth *GM* to 1 part in 10^6, the effect could be precisely mapped into the lunar mass. The various Ranger probes that struck the moon broke the earth–moon mass correlation and directly and independently determined the lunar mass from its effect on the spacecraft orbit during the last few hours before impact. The agreement of all solutions is shown in figure 7.

The atmosphere of Mars has been analyzed from data recorded just before occultation of the spacecraft signal by the planet.[9] The integrated Doppler residual plot in figure 8 shows the definite effects of both the Martian ionosphere and atmosphere. The data measure directly the effects of refraction and retardation in Doppler phase of the signal as it passes through the various atmospheric layers.

Two checks on the accuracy of the theoretical lunar ephemeris were obtained with data from Lunar Orbiter and the landed Surveyor. We used Orbiter to check Wallace J. Eckert's[10] corrections to the Brown Lunar Ephemeris (up to 2 km in the radial-distance parameter was required to bring this coördinate to the precision of Brown's theoretically developed accuracy). With the Lunar Orbiter Doppler data, it was possible to establish the spacecraft's position, relative to the moon, independently of any ephemeris error. Then, with an independent spacecraft-ranging system, residuals were established between the ephemeris position of the moon and that determined from the data[11] as in figure 9. These residuals were approximately in agreement with Eckert, but there remained 300–400-meter differences that demanded explanation.

Turning to the landed-Surveyor data, we observed that the residuals

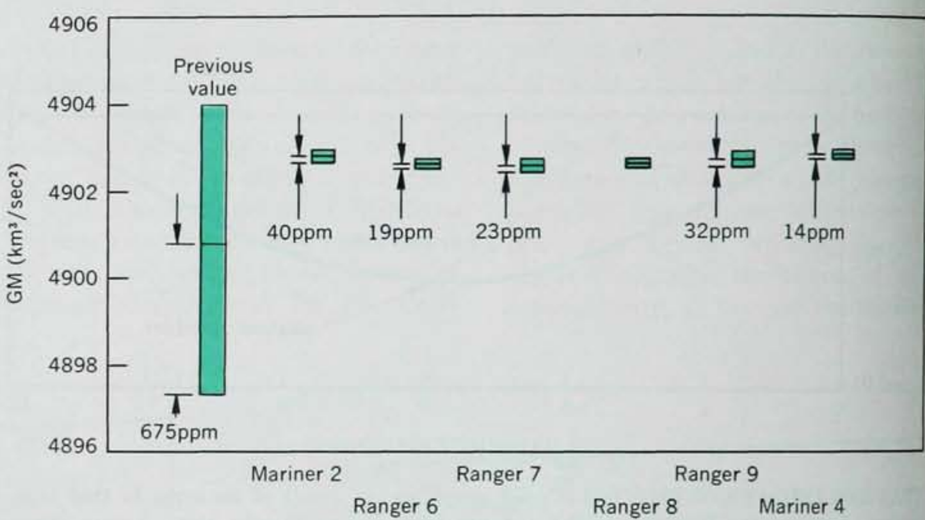

LUNAR MASS, in terms of *GM*, from Doppler data of six spacecraft. —FIG. 7

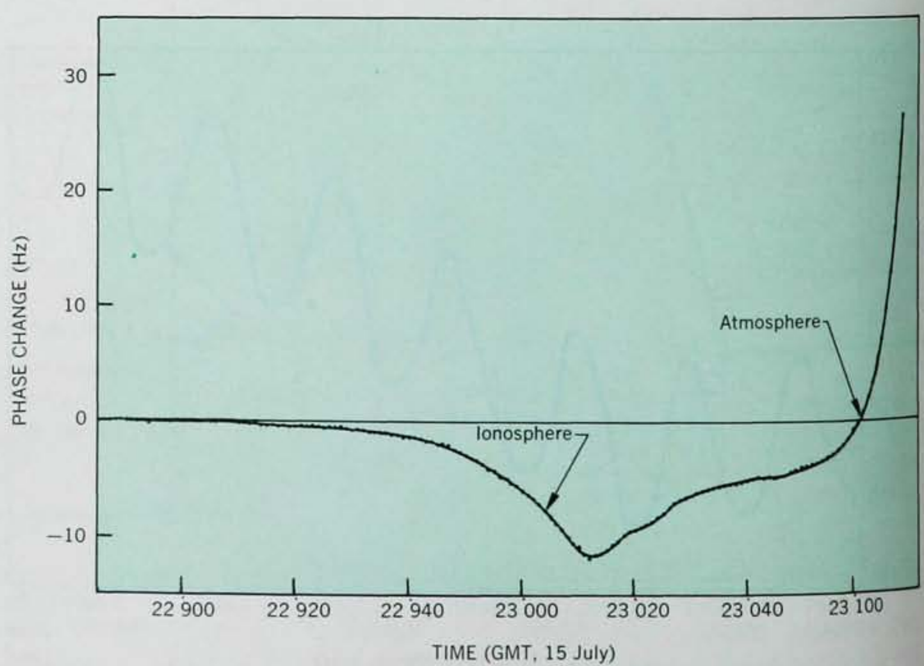

OCCULTATION EXPERIMENT performed on 4 March when Mariner 4 went behind Mars. The data show the effects of refraction and retardation upon the tracking signal, resulting from the Martian atmosphere and ionosphere. —FIG. 8

had a low-amplitude 14-day periodic effect (figure 10). About the same time, a new numerical integration of the theoretical ephemeris of the moon was made available through research at JPL.[12,13,14] Substitution of this improved ephemeris reduced the Lunar Orbiter residuals to 100 meters and significantly reduced the 14-day Surveyor range-rate residuals as well. The remaining short-period (diurnal) effects in the Surveyor residuals are presently unknown, but thought to be primarily caused by the earth's troposphere and ionosphere. The remaining 100 meters in the Lunar Orbiter range–ephemeris residuals result from variations in the local lunar gravity field, which is under extensive analysis and is directly related to the mascon discovery.[15]

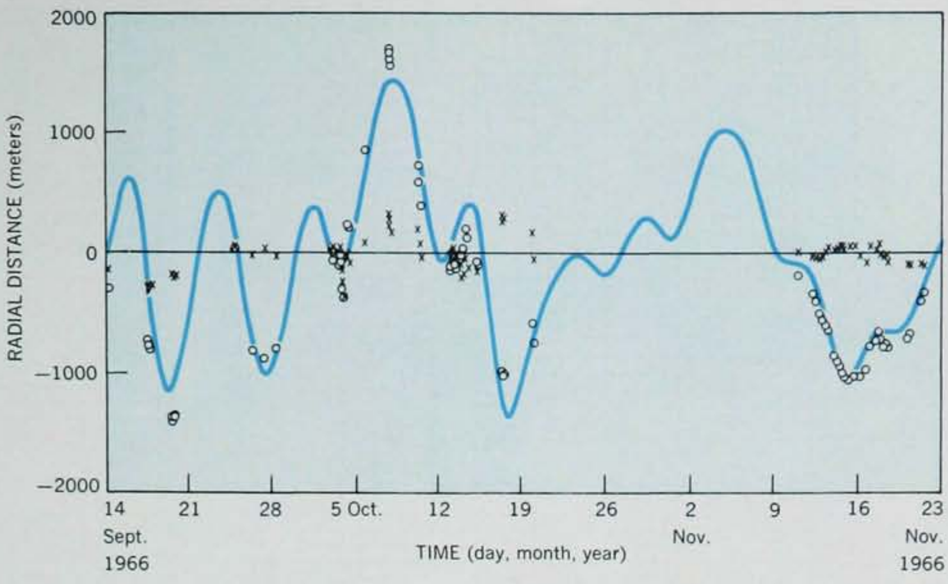

LUNAR EPHEMERIS or accurate position of the moon. Raw data (open circles) and corrected data (crosses) from Lunar Orbiter are here compared with Eckert's corrections to Brown's theoretical curve, for the lunar position. —FIG. 9

Mascons

Because of the lack of an apparent pattern in the large Lunar Orbiter residuals, the validity was repeatedly under question. Processing of the data led to inconsistent determinations of the low-order terms in the lunar gravity field. We now know that 15th- to 20th-degree spherical harmonics are required to describe the major local gravity anomalies. Figure 11 shows the strong systematic effects in only a short 90-minute arc of data, during which the spacecraft passed from the south to the north pole. The variations in the velocity residuals are more than two orders of magnitude above the noise level, and the information content is by no means marginal. To see this 50-mm/sec effect, we have to remove orbital velocity rates of 2×10^6 mm/sec. The small, 50-mm/sec, velocity variations integrate to 10 or 20 meters at the lunar distance of 4×10^8 meters.

To obtain a gravimetric map of the lunar nearside, we processed 74 consecutive orbits from Lunar Orbiter 5. During this time, the moon rotated beneath the essentially inertial spacecraft-orbit plane, thereby mapping the nearside between ± 60 deg of longitude in steps of approximately 1.5 deg per orbit. As shown in figure 11, the residuals were very prominent. They represent the remaining line-of-sight velocity in the observational data, after the effects of the theoretical motion of the moon, tracking stations, and the selenocentric spacecraft motion as perturbed by a triaxial moon, the sun and major planets, have been removed. The residuals themselves were then

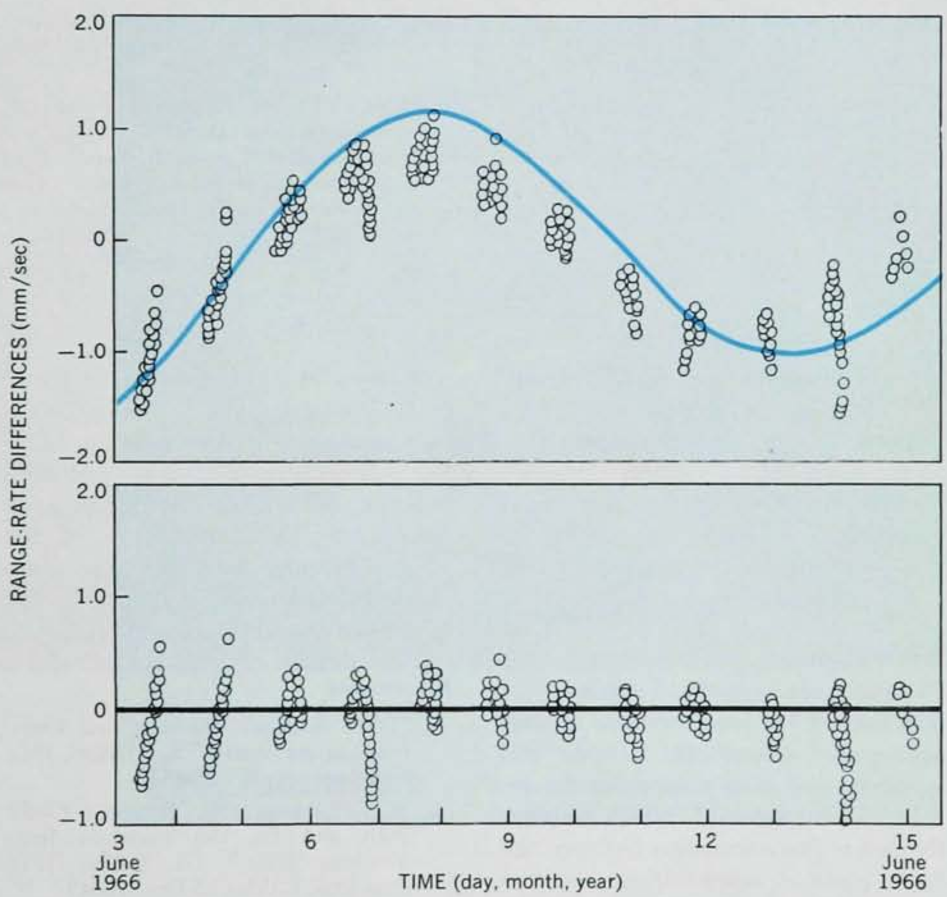

SURVEYOR DOPPLER RESIDUALS. The 14-day periodic difference (upper graph) between the observations and Brown's calculated ephemeris was eliminated when an improved theoretical ephemeris was substituted for Brown's data. —FIG. 10

fitted with sets of spline-fit (patched) cubic polynomials to smooth the data and permit stable numerical differentiation to obtain the desired acceleration data that would be a measure of the gravitational variations.

It should be noted that the least-squares fitting processes that we employed tend to reduce the amplitude of larger perturbations and even introduce erroneous compensating second-order variations. Despite sim-

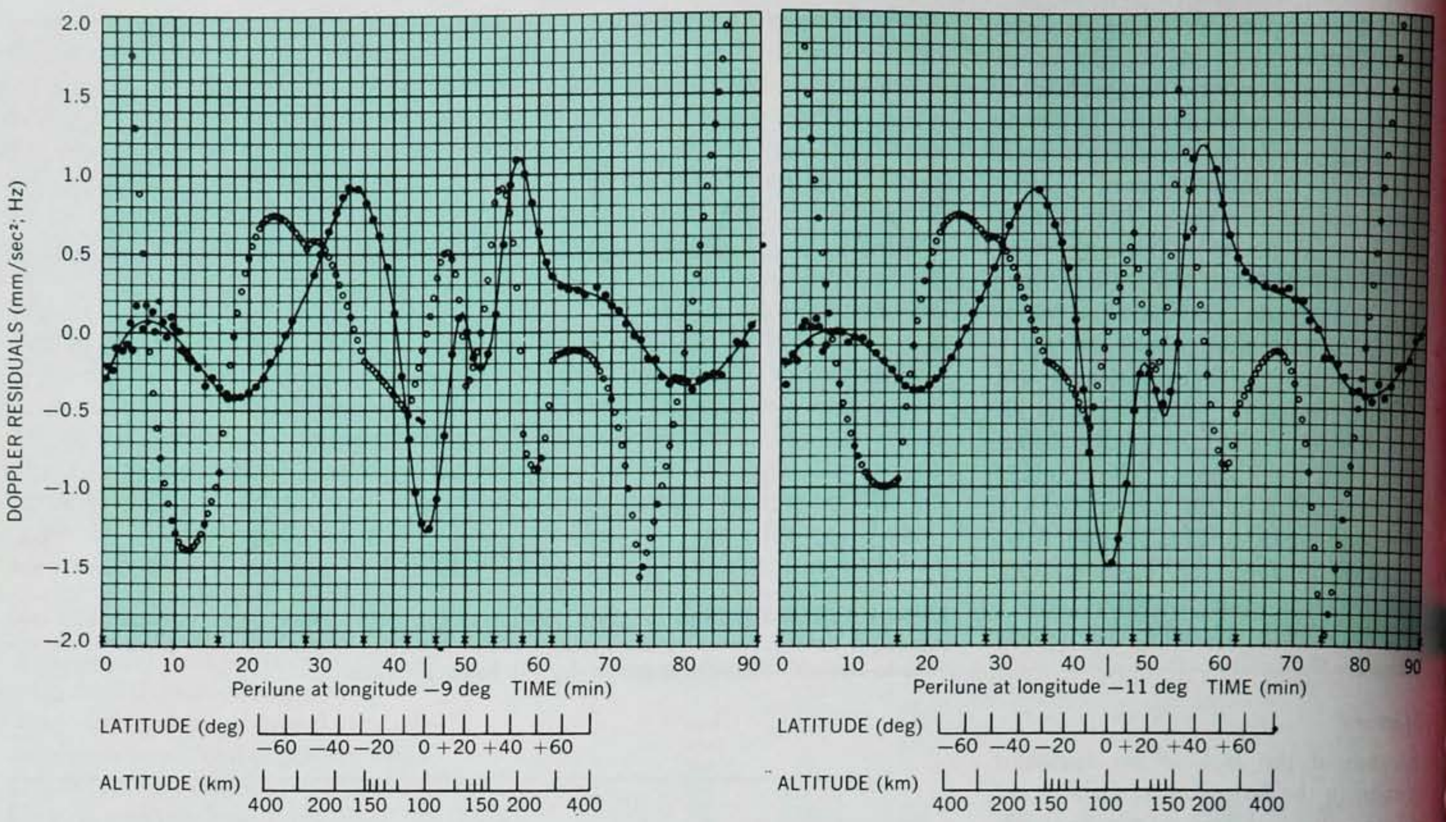

VARIATIONS IN VELOCITY for 90-minute passes of Lunar Orbiter 5-C during orbits 45 (left) and 46 (right). Asterisks are raw Doppler residuals (in Hz, where 1Hz is equivalent to 65 mm/sec) with a patched cubic fit drawn through them. Open circles are normalized acceleration (mm/sec²), and crosses are patched cubic break points. These variations result from major local gravity anomalies, or mass concentrations in the moon as shown on the left side of figure 1. —FIG. 11

plifying assumptions regarding geometry, fit and the employment of an approximate normalization function to account for differences in spacecraft altitude, we obtained a usable gravimetric map of the lunar nearside between longitudes ±60 deg and latitudes ±50 deg.

Lunar maps

Plotting these normalized accelerations on a map of the lunar nearside at their appropriate selenodetic latitude and longitude and then contouring the results yielded figure 1, which displays the one-to-one correlation between the large positive accelerations and the ringed seas Imbrium, Serenitatis, Crisium, Nectaris, Humorum and Aestuum. Subsequent improvements in the technique have extended the gravimetric map to longitudes ±110 deg revealing further mascons in the remaining ringed seas, Orientale, Smythii, Grimaldi and Humboltianum, bringing the verified total to ten.

Discovery of these unexpected gravity-anomaly patterns has been the latest dividend in a successful program of scientific investigation based on the processing of this highly precise Doppler-tracking data.

Future investigations with the Mariner spacecraft will involve continued analysis on the Mars atmosphere and ionosphere, an investigation of the Martian gravity field and a solar-occultation experiment leading to a test of general relativity.

References

1. "DSIF S Band Tracking and Communications System" **2**, ED-256, JPL, Pasadena, Calif. (1965).
2. W. L. Sjogren et al, "Ranger 6 Flight Path and Its Determination from Tracking Data," TR 32-605, JPL, Pasadena, Calif. (15 Dec. 1964).
3. W. R. Wollenhaupt et al, "Ranger 7 Flight Path and Its Determination from Tracking Data," TR 32-694, JPL, Pasadena, Calif. (15 Dec. 1964).
4. W. G. Melbourne, J. D. Mulholland, W. L. Sjogren, F. M. Sturms Jr, "Constants and Related Information for Astrodynamic Calculations, 1968," TR 32-1306, JPL, Pasadena, Calif. (15 July 1968).
5. N. A. Mottinger, "Status of DSS Location Solutions for Deep Space Probe Missions III: Recent Achievements Using Mariner 4, Mariner 5 and Pioneer 7 Data," in Space Programs Summary 37–56, **2**, JPL, Pasadena, Calif.
6. "Constants and Related Data Used in Trajectory Calculations at the Jet Propulsion Laboratory," TR 32-273, JPL, Pasadena, Calif. (1 May 1962).
7. J. D. Anderson, G. W. Null, C. T. Thornton, "The Evaluation of Certain Astronomical Constants from the Radio Tracking of Mariner 2," in *Progress in Astronautics and Aeronautics* **14**, Academic Press, New York (1964).
8. G. W. Null, H. J. Gordon, D. A. Tito, "The Mariner 4 Flight Path and Its Determination from Tracking Data," TR 32-1108, JPL, Pasadena, Calif. (1 Aug. 1967).
9. A. J. Kliore, D. L. Cain, G. S. Levy, V. R. Eshleman, G. Fjeldbo, F. D. Drake, Science **149**, 3689 (1965).
10. W. J. Eckert, M. J. Walker, D. Eckert, Astron. J. **71**, 314 (1966).
11. J. D. Mulholland, W. L. Sjogren, Science **155**, 3758 (1967).
12. F. M. Sturms Jr, "An Integrated Lunar Ephemeris," Space Programs Summary 37–48, **2**, JPL, Pasadena, Calif. (30 Nov. 1967).
13. J. D. Mulholland, C. J. Devine, Science **160**, 874 (1968).
14. C. N. Cary, W. L. Sjogren, Science **160**, 875 (1968).
15. P. M. Muller, W. L. Sjogren, Science **161**, 680 (1968). □